Dielectrophoretic alignment of Al2O3/PDMS composites: Enhancement of thermal and dielectric properties through structural sedimentation analysis

Omar Zahhaf, Giulia d'Ambrogio, Minh-Quyen Le, Gildas Coativy, François Grasland, Pierre-Jean Cottinet, Jean-Fabien Capsal

Version of Record: https://www.sciencedirect.com/science/article/pii/S0264127521006894
Manuscript_294fd25984293adc6c7577412bb3d811

Dielectrophoretic Alignment of Al_2O_3/PDMS Composites: Enhancement of Thermal and Dielectric Properties Through Structural Sedimentation Analysis

Omar Zahhaf [1], *Giulia D'Ambrogio* [1], *Minh Quyen Le* [1], *Gildas Coativy* [1], *François Grasland* [2], *Pierre-Jean Cottinet* [1*], *and Jean-Fabien Capsal* [1]

[1] Univ. Lyon, INSA-Lyon, LGEF, EA682, F-69621, VILLEURBANNE, France.

[2] GETELEC, 78530 Buc, France

*Corresponding author: pierre-jean.cottinet@insa-lyon.fr

Abstract: Thermally conductive composites have emerged as a promising lead towards a more suitable and efficient alternative for thermal management. Their advantage lies in the coupling of different but complementary properties such as thermal conductivity for heat dissipation and flexibility for fitting surface irregularities. However, such materials consisting of ceramic fillers dispersed in a polymeric matrix generally suffer from particle sedimentation that ultimately affects their performance. Therefore, the overall properties of these composites can be further enhanced through structural improvements. Dielectrophoretic alignment has proven to be an effective and practical method to reach better structures that eventually improve the composites' properties. This paper focuses on the enhancement of thermal and dielectric properties of Al_2O_3/PDMS composites through dielectrophoretic alignment. A novel method for measuring sedimentation effects is presented with a particular emphasis on the role of dielectrophoresis in counteracting those undesired effects. The influence of the relevant parameters such as the amplitude and frequency of the applied electric field is analyzed in order to draw the best structuring conditions. The thermal conductivity as well as the dielectric response are then compared between structured and unstructured composites. This comparison revealed a significant structural improvement that led to enhanced thermal conductivities while keeping the insulating properties unchanged.

1 Introduction

The last decades have witnessed a drastic development of the field of electronics. This gave rise to several challenges that must be met in order to perpetuate this evolution [1,2]. Indeed, as predicted by Moore's law, the number of integrated electronic components have not ceased to increase [3]. For instance, today's most elaborate microprocessors commercially available contain more than thirty billion transistors. However, the pursue of performance through miniaturization and complexity has led to a significant power-dissipation that affects not only the reliability and lifespan of the operating components but also the performance that is sought to be improved [4]. It is therefore crucial to develop innovative and increasingly efficient materials for thermal management [5].

Temperature increase and heat flux within electronic devices can be managed through several approaches. Heat sinks, typically made of metallic materials are the traditional way to dissipate heat within electronic devices. However, this method alone is no longer considered to be the most efficient one. Because of the abundance of free electrons, metallic materials usually exhibit high thermal conductivities [6]. Nonetheless, their stiffness and surface roughness inevitably lead to a poor thermal contact between the mating surfaces which tends to reduce significantly the heat transfer [7]. Moreover, most of metallic materials suffer from a high coefficient of thermal expansion resulting in thermal stress with temperature variations [6,8]. Thus, a new approach regarding heat dissipation is needed to address this matter.

Polymeric composites with high thermal conductivity have attracted a strong interest over the last years in both industrial and research fields [9–15]. Their versatility, ease of processing, light weight and low cost make them a more promising and attractive alternative. By choosing an adequate coupling of the matrix and fillers, the properties of the developed composite can be easily shaped to match its dedicated application. For instance, aerospace and automotive industry, energy storage and conversion systems would require high thermal stability, good mechanical flexibility, low dielectric permittivity along with electrical insulation [6,12,16,17]. Thus, given these requirements, ceramic fillers such as AlN, BN or Al_2O_3 would be the most suitable alternative to the conventional materials [11], [18]. Carbon-based fillers for instance are widely used for their excellent thermal conductivity [19]. However, their electrical conductivity limits significantly their field of application, particularly regarding thermal management in

microelectronics [20,21]. Since flexibility is a necessary element for the intended application, the use of elastomeric polymers for the fabrication of composites is indispensable [22]. Among commercially available elastomers, Polydimethylsiloxane (PDMS), is one of the most widely used due to its interesting properties with respect to its counterparts. Indeed, PDMS offers good mechanical behavior [23] and high thermal stability [24], low dielectric constant and thermal expansion coefficient, as well as excellent dielectric strength. Furthermore, this elastomer is extremely flexible, cost effective and adaptable to additive manufacturing. These features make PDMS one of the most appropriate candidates for the development of stretchable smart materials in various applications (medical instrumentation, structural health monitoring and so on) [25–28].

In an isotropic structure, the thermal conductivity of a polymeric composite is strongly dependent on the filler loading level. At a low volume content, the fillers are isolated from each other, separated by polymer that acts as a thermal barrier [29,30]. As the loading level increases, the fillers tend to form thermally conductive pathways which, beyond a certain filler content, grow into a single three-dimensional interconnected network. The overall thermal conductivity then exhibits a significant leap due to a more efficient heat transfer [29]. Thus, highly thermally conductive composites can be obtained through very high filler concentrations [31–33]. However, filler overloading leads to a significant degradation of the mechanical properties as well as a poor processability and high cost [10,32,33]. Therefore, achieving high thermal conductivities while simultaneously maintaining good mechanical properties remains a daunting challenge.

In this context, electric field induced particle alignment represents an efficient and promising way to increase the connectivity between the fillers within a composite material [31,34,35]. Indeed, this process known as dielectrophoresis, utilizes induced dipole-dipole interactions between electrically insulating particles to align a random dispersion into a chain-like structure [31,36,37], [38]. This results in a field-structured anisotropic composite exhibiting unidirectional thermally conductive pathways which minimize the thermal resistance along the field direction. In general, dielectrophoresis presents the advantage of being able to structure, along the electric field's direction, any dielectric filler within a polymeric matrix as long as the two phases have a dielectric contrast with one another. This statement is hardly true for other methods of structuring without a special filler surface modification or coating. Among them, acoustophoresis, based on ultrasonic standing waves, has been used for noncontact particle manipulation. However, an intense acoustic field may cause the composite blend to heat which can modify its viscosity. Thermophoresis needs a temperature gradient across the sample, while electrophoresis requires an electric field with direct electrode contact that induces Joule heating [39]. The process is fundamentally different in the case of dielectrophoresis, where direct electrode contact is not necessary to drive particle's movement. Magnetophoresis might be an effective alternative to dielectrophoresis, in which the alignment occurs under magnetic field instead of electric field. However, this method commonly entails the presence of a magnetic coating layer. For instance, Kim *et al.* successfully aligned AlN@Fe_3O_4 fillers in an epoxy matrix through a magnetic field [40]. Similarly, Xiang *et al.* developed magnetically structured composites where no coating layer is needed [41]. However, this method is only applicable to materials with strong ferromagnetic properties (like bulk Fe_3O_4 or Nickel), not to dielectric fillers like AlN or Al_2O_3. Nonetheless, the thermal conductivity of ferromagnetic materials is intrinsically lower than that of alumina, which limits the potential enhancement of the effective thermal conductivity of the composite.

This paper deals with dielectrophoretic alignment of spherical alumina particles embedded into a silicone matrix, which is considered to be the most suitable choice for manipulating dielectric fillers. A novel method is proposed, for the first time, to assess sedimentation effects through the thermal properties of the composites. To date, measuring the thermal conductivity of the sedimented composites, regardless of the sample's configuration (0-3 or 1-3 connectivity), has been rarely reported. The developed approach, with a particular focus on the role of dielectrophoresis, allows to demonstrate how the gravitational force can be compensated to limit the particle's sedimentation within the polymeric blend. The success of the process is considerably affected by several key parameters comprising the electric field's amplitude and frequency as well as the loading level of the composite. The structural dependence of those parameters is therefore correlated to thermal and dielectric properties as well as the sedimentation state of the composites. The most appropriate parameters to structure Al_2O_3/PDMS composites are chosen with the aim of comparing the random 0-3 samples and their aligned 1-3 counterparts. The enhancement of thermal properties and dielectric behavior through dielectrophoretic alignment is then thoroughly discussed.

2 Theoretical Background

Dielectrophoresis (DEP), a term first introduced by Pohl [42], denotes the motion of dielectric polarized suspensoid particles resulting from interactions between their dipoles and the applied nonuniform electric field. The acting force underlain by those interactions is known as the dielectrophoretic force. It is dependent on the amplitude and frequency of the external electric field as well as the dielectric properties of the particles relative to their medium. For spherical particles, this dependence can be expressed mathematically as follows [43][44]:

$$F_{DEP} = 4\pi . R^3 . \varepsilon_0 . \varepsilon_m . Re[CM(\omega)] . (E \cdot \nabla)E \qquad \text{Eq. 1}$$

where R is the particles' radius, ε_0 and ε_m are the dielectric constants of the vacuum and the medium respectively, E is the electric field and $Re[CM(\omega)]$ is the real part of the Clausius-Mossotti factor which indicates the dielectric properties of the particles in contrast with their medium. The $Re[CM(\omega)]$ term is driven by the frequency, the relative permittivity as well as the electrical conductivity of the phases involved. $Re[CM(\omega)]$ is given by [43] :

$$Re[CM(\omega)] = \frac{\omega^2(\varepsilon_p - \varepsilon_m)(\varepsilon_p + 2\varepsilon_m) + (\sigma_p - \sigma_m)(\sigma_p + 2\sigma_m)}{\omega^2(\varepsilon_p + 2\varepsilon_m)^2 + (\sigma_p + 2\sigma_m)^2} \qquad \text{Eq. 2}$$

where σ_p and σ_m are the electrical conductivities of the particles and the medium, respectively. When the polarization of the particles is different from the one of the surrounding medium, the electric field is locally distorted and each particle is then subjected to a non-uniform electric field from its neighboring particles [45]. This gives rise to attraction/repulsion forces among the particles, moving them into columnar-like structures. The energy of those interactions is expressed as:

$$U(r, \theta) = -\left(\frac{\mu^2}{\varepsilon_m r^3}\right) . (3\cos^2\theta - 1), \qquad r \geq 2a \qquad \text{Eq. 3}$$

where r is the inter-particle distance, θ is the angle between the vector parallel to r and the electric field's direction, μ is the induced dipole moment, ε_m is the dielectric constant of the medium, and a is the radius of the particles. According to Eq. 3, the interaction between particles would be attractive for θ below 54.7 ° and repulsive otherwise.

The above equations give a physical understanding of relevant parameters that play a significant role in the process and show how they impact the resulting structure. Eq. 1 describes the role of the dielectrophoretic force on the electric field's amplitude while Eq. 3 indirectly highlights the frequency dependence of the dipole-dipole interactions. On one hand, the energy of those interactions is proportional to the square of the induced dipole moment, i.e., relating to the particle's polarizability. On the other hand, the real part of the polarizability (often noted α') is inversely proportional to the square of the angular frequency. Therefore, an increase in the frequency induces a decrease in the polarizability that might weaken the dipole interactions between particles. Observations obtained from microscopic imaging techniques together with experimental results through the dielectric and thermal measurements (cf. Section 4) allow to confirm the structuration behavior of the predicted model.

Following the nomenclature introduced by Newnham [46], the connectivity of a diphasic composite can be described through the number of dimensions in which each phase is self-connected. For instance, a 0-3 connectivity pattern denotes isolated fillers surrounded by a three-dimensionally connected matrix. On the other hand, a 1-3 structure refers to one-dimensionally connected fillers in a three-dimensional matrix [46].

It is worth noting that randomly dispersed particles within a continuous matrix do not necessarily imply a 0-3 connectivity, e.g., in case of percolated and randomly dispersed fillers. Similarly, spherical aligned particles within a matrix are usually separated by thin layers of polymer, which in this case, cannot be considered as a 1-3 structure. In this paper, for the sake of clarity, composites with randomly dispersed particles will be noted as 0-3 structures whereas the ones with aligned fillers will be referred to as 1-3 structures.

3 Material Preparation and Characterization Method

3.1 Material preparation

Alumina particles, available at Showa Denko America, Inc., were used as thermally conductive fillers. These spherical particles, shown in **Figure 1(A)**, have a density of 3.79 g/cm^3, a specific surface area of 0.14 m^2/g and a median size of 20.8 µm. **Figure 1(B)** shows their cumulative and differential size distribution.

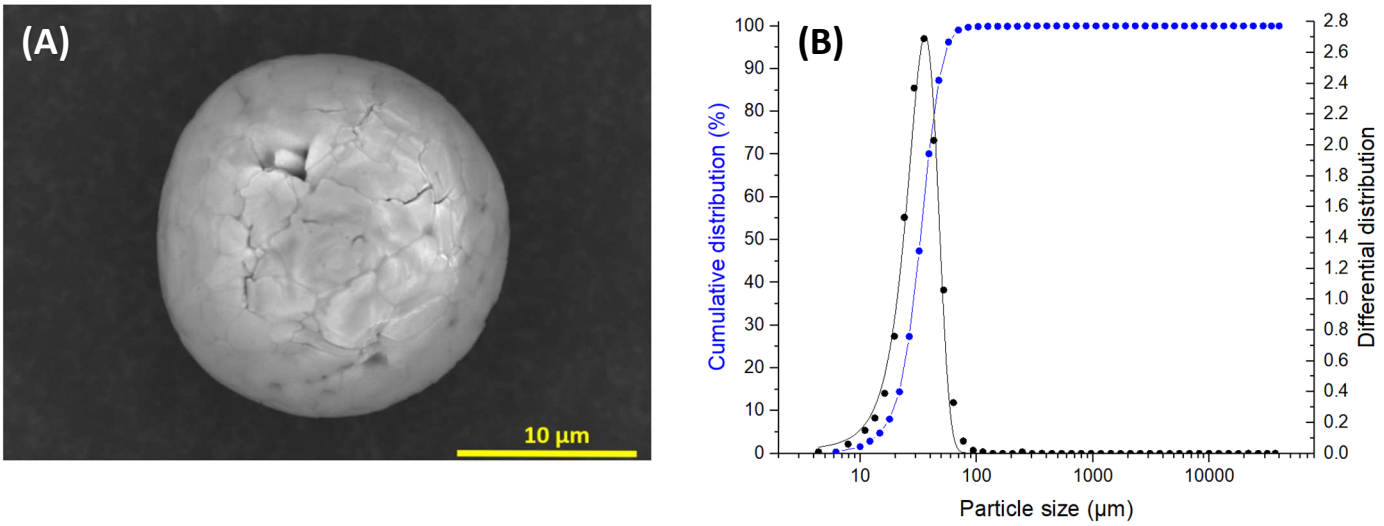

Figure 1 : *(A) Scanning Electron Microscopy (SEM) of 20 µm spherical alumina particles, (B) Cumulative and differential distribution as function of particle size*

The silicone elastomer (Polydimethylsiloxane), available in Sigma-Aldrich®, was used as polymeric matrix. It is a two-part liquid including a base and a curing agent mixed at a 10:1 ratio. The polymerization begins when curing agent is added to the base. As the curing progresses, the viscosity increases until the material becomes a "cured" flexible elastomer.

The Al_2O_3/PDMS composites are prepared by adding the desired volume fraction of alumina particles to the PDMS base to avoid local polymerization due to the sonication process. The blend is mechanically mixed for 5 min until it is visually homogenous, then sonicated for 5 min via an ultrasonic probe (Hielscher Ultrasound Technology, UP400S). Next, the curing agent is added and the blend is further mixed for 5 min using an overhead stirrer. Subsequently, the resulting homogenous compound is poured into the bottom part of two identical molds shown in **Figure 2.** The whole system is subjected to a 5-mbar vacuum for 30 min to remove air bubbles entrapped during the mixing process. The first mold, used to obtain the 1-3 composites, is connected to a high-voltage power amplifier (Trek Model 20/20C) and placed inside a Vötsch VTM 7004 climate chamber. An AC sinusoidal electric field is applied at 25°C for 20 min after which the temperature is gradually increased to 120°C. The structured sample is cured under dielectrophoresis for one hour at 120°C. The second mold, intended for elaborating 0-3 samples, follows the same protocol (i.e., 120°C during 1 hour) but without applying the electric field. After the curing process, both the 0-3 and 1-3 composites are cooled down at room temperature, carefully unmolded and prepared for characterization.

It is interesting to note that in the dielectrophoresis process described above, the electric field is applied first at room temperature to trigger the alignment of the fillers while the matrix is still not cured. The electric field is then maintained during polymerization to conserve the structure in its aligned state. Therefore, as soon as the curing starts, the columns have already been in the final stages of their aligned configuration. In this situation, adjusting the curing time will not have an impact on the resulting structure. On the contrary, if the electric field was applied after the polymerization has started, the curing time would have an impact on the structure but probably not in a way that will directly change the width of the columns. It will result instead in "incomplete" structures as the curing time decreases.

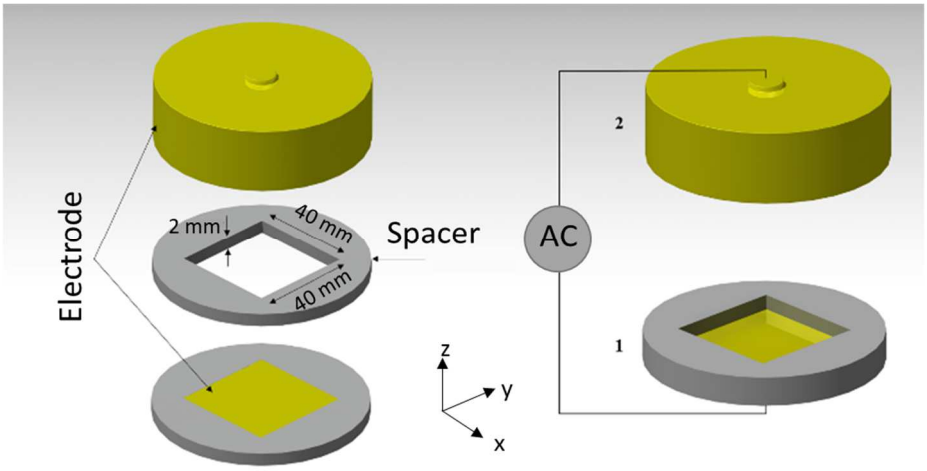

Figure 2 : *Schematic of the mold used to structure the composites along the "z" direction. (1) represents the bottom part where the non-cured composite is poured. (2) represents the top electrode used a mass keeping the sample under compression stress.*

3.2 Characterization method

The filler alignment in uncured PDMS is monitored by an optical digital microscope (Dino-Lite AM7915MZT). The Al_2O_3/PDMS blend is placed between two electrodes inside a transparent mold made of Polycarbonate. The mold was designed such that the electrodes would be orthogonal to the vertical "z" axis. Consequently, gravitational effects were considered in the parameters' analysis as described in the next section.

An alternative method to observe the particle alignment for higher filler content is through Scanning Electron Microscopy (SEM) Analysis. The samples' cross-sectional morphology was characterized using an SEM (HITACHI FlexSEM 1000II), with a magnification of ×70.

The dielectric spectroscopy of the Al_2O_3/PDMS composites was carried out using a Solartron Analytical Dielectric Interface System (model 1296A), coupled with a high frequency response analyzer. The dielectric spectra of the 0-3 and 1-3 composites were acquired at ambient temperature via a sample holder (AMETEK, 12962A), on which was applied an AC electric field with an amplitude of 1 V_{rms} and a frequency range of 0.1 Hz to 1 MHz.

The thermal conductivity of the samples was measured along the "z" direction at room temperature using the modified transient plane Source (MTPS) method (TCI analyzer, C-THERM). It consists in using a unilateral interfacial thermal reflectance sensor that generates a constant heat flow through the sample. The measurement of temperature variations ensures a detailed overview of the thermal properties of the samples [47].

4 Results and Discussion

In order to better understand the physics behind the dielectrophoretic alignment, it is crucially important to identify the relationship between the major forces acting towards and against chain-like structures. As discussed in section 2, the field-induced dipolar interactions resulting from the dielectric contrast between the two phases is at the foundation of particle alignment [48]. Acting against those interactions stand the "misaligning" forces which are dominated to a large part by drag force and gravity. On one hand, the drag force is related to the viscosity of the uncured silicone matrix in addition to the fillers' form factor and loading level. However, as the drag force increases along with the filler content, it is counterbalanced by the particle proximity that enhances the dipolar interactions as well. On the other hand, the gravitational forces are constantly moving the particles downwards, thus leading to sedimented structures and significantly decreasing the overall properties of the composite (e.g., thermal, electrical, dielectric behavior). These often-overlooked aspects of dielectrophoresis will be reviewed through this discussion, since favorable structures can arise only when aligning interactions overbalance the magnitude of the misaligning forces.

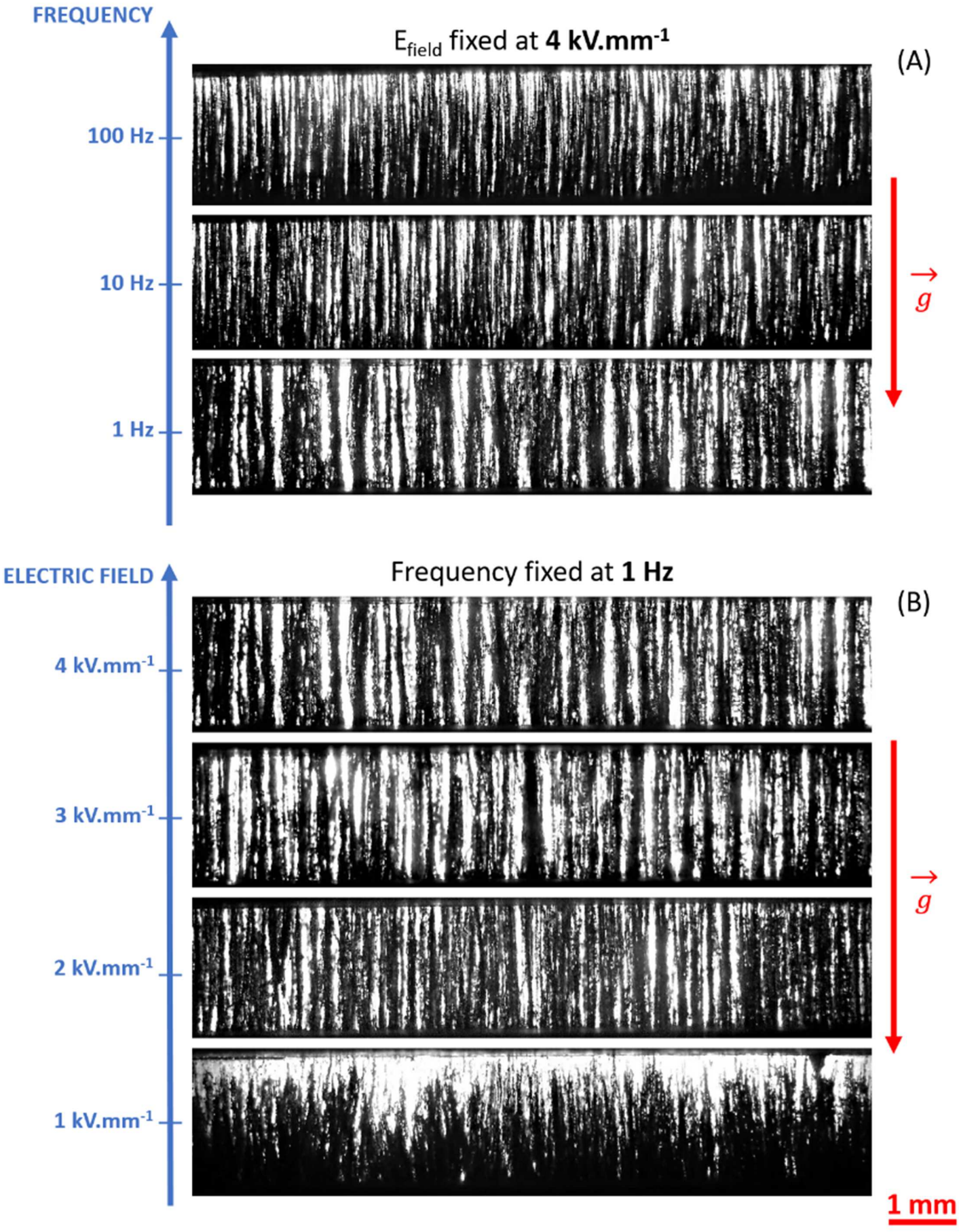

Figure 3 : *Transmission optical microscopic observations of uncured Al_2O_3/PDMS at 2.5 vol% after 30 min: (A) Frequency dependence analysis from 1 Hz to 100 Hz at a fixed electric field of 4 kV.mm^{-1}. (B) Electric field dependence analysis from 1 kV.mm^{-1} to 4 kV.mm^{-1} at a fixed frequency of 1 Hz. (Black represents the particles, white represents the matrix; $\vec{g}$ denotes the gravitational acceleration vector, which is in the vertical downward direction).*

It is worth noting that higher loading level of the composite can lead to better thermal performance. However, in microscopic imaging study, composites with low filler content makes observation easier. It has been pointed out in Zhang *et al*. that the formation of particle in aligned chains via SEM image is not evident with a loading level above 10 vol% [26]. As the loading level increases, the movement resistance does indeed increase along with it. However, the space barrier between fillers decreases as more particles occupy the same volume within the matrix. In that case, the dipole interactions between fillers, which are inversely proportional to the cube of the inter-particle distance (cf. Eq. 3), are enhanced with respect to an increase in the volume content. As a matter of fact, the microscopic observations on low-filler-content composites could not entirely represent the complexity of their behavior at a higher content under an applied electric field, as the magnitude of many physical forces changes with the increasing loading level. However, the principal goal of microscopic observations involved in this study is aimed to figure out how the relevant parameters (electric field's magnitude and frequency) could affect the structuration of material when being subjected to dielectrophoretic treatment. Although the magnitude of the applied field might change as the filler content increases, it should theoretically stay consistent with higher loading level. In this context, both high and low frequencies induce the fillers to align themselves into a chain-like structure. However, the width of the individual columns is highly dependent on the frequency of the applied electric field.

4.1 Parameter Dependence Analysis

It has been established that the strength of the dielectrophoretic force depends strongly on the medium, the nature and morphology of the particles. The frequency and amplitude of the applied electric field matter as well. Through different characterization tests (i.e., imaging, dielectric, thermal), this section aims at determining the best set parameters of the input voltage. Moreover, it will be demonstrated that an appropriate tuning of those parameters compensates for the undesired effects of gravity.

According to Eq. 1, the higher the electric field's amplitude, the higher the dielectrophoretic force as well as the dipole interactions that enables the creation of anisotropic structures. From a practical point of view, however, high amplitudes also lead to a high breakdown probability. This is due to the fact that the local electric field is enhanced at the interfaces between the particles and the matrix, and the mobility of particles favored within the uncured matrix during dielectrophoretic process. The electric field's amplitude is thus limited by the polymer's dielectric strength and its optimal value can be determined based on the best compromise between the structuration efficiency and the breakdown strength. In the following experiment, electric fields greater than $4 kV.mm^{-1}$ will be not considered to prevent any sample damage.

In addition, frequencies lower than 1 Hz are not considered neither as they would lead to inefficient structuration. Indeed, at very low frequencies, the ionic species have enough time to redistribute themselves into charge layers near the electrodes, provoking a voltage drop and inhibiting chain formation as a consequence [49]. Moreover, low enough frequencies would allow particle accumulation near the electrodes. As the amplitude of the particle oscillations increases with the decreasing frequency, the dielectrophoretic force becomes higher than the dipole interactions when the particle approaches the electrodes. This result in trapping the particle near the electrodes and as a result, the disruption of the columns formation.

4.1.1 Real-time Optical Microscopy (OM) Monitoring

With the aim of better understanding the dependence of the dielectrophoretic force on the frequency and amplitude of the applied electric field, the kinetics of particle movement were monitored in real-time through transmission optical microscopy (OM). Various frequencies (i.e., 1 Hz, 10 Hz, 100 Hz) and electric field's amplitudes (i.e., 1, 2, 3 and $4 kV.mm^{-1}$) were analyzed at low filler content of 2.5 vol% so that light could travel through a 2 mm blend thickness. Images with a magnification of ×38 were recorded and clearly show the formation of aligned particle chains along the field direction.

The first relevant parameter considered for the dielectrophoretic experiment is the frequency. A practical test is carried out on 2.5 vol% Al_2O_3/PDMS composites under the same electric field of 4 $kV.mm^{-1}$ amplitude but with different frequencies. As indicated in **Figure 3(A)**, at a low frequency of 1 Hz, a favorable structure with coarse continuous columns is observed. As the frequency increases, thinner structures start to emerge, and sedimentation effects become more and more pronounced.

As discussed in Eq. 1, the dielectrophoretic force is proportional to the amplitude of the applied electric field. **Figure 3(B)** highlights the electric field dependence of 1-3 structured samples. Under low-voltage excitation of

1 kV.mm^{-1}, the particles align themselves in a non-percolated chain like structure suggesting that the dielectrophoretic force is not strong enough to counterbalance the particles' weight. In other words, particle sedimentation occurs nonetheless. Under 2 kV.mm^{-1}, the chains bridge the electrodes with a higher particle concentration at the bottom electrode. Although the electric field is sufficient to obtain a percolated structure, it is not high enough to suppress all signs of sedimentation. A further increase in the electric field (i.e., 3 and 4 kV.mm^{-1}) leads to coarser structures and more homogenous columns, where sedimentation is completely compensated.

Therefore, it can be deduced that the frequency and the amplitude of the applied electric field affect not only the size of particle columns but also the degree of sedimentation caused by the gravitational force. To provide a more convincing conclusion, sedimentation effects were further investigated through other characterization tests including SEM analysis, thermal conductivity, and dielectric spectroscopy measurements.

4.1.2 Scanning Electron Microscopic (SEM) Observations

To further investigate the conclusions of the previous OM analysis, SEM observations were performed on Al_2O_3/PDMS composites subjected to the same conditions of dielectrophoretic structuring. The filler content was fixed at 10 vol%, which stands between the real-time microscopy conditions and the loading levels typically used for thermally conductive composites. **Figure 4** shows the cross-sectional SEM micrographs of the frequency dependence analysis at a fixed electric field of 4 kV.mm^{-1}.

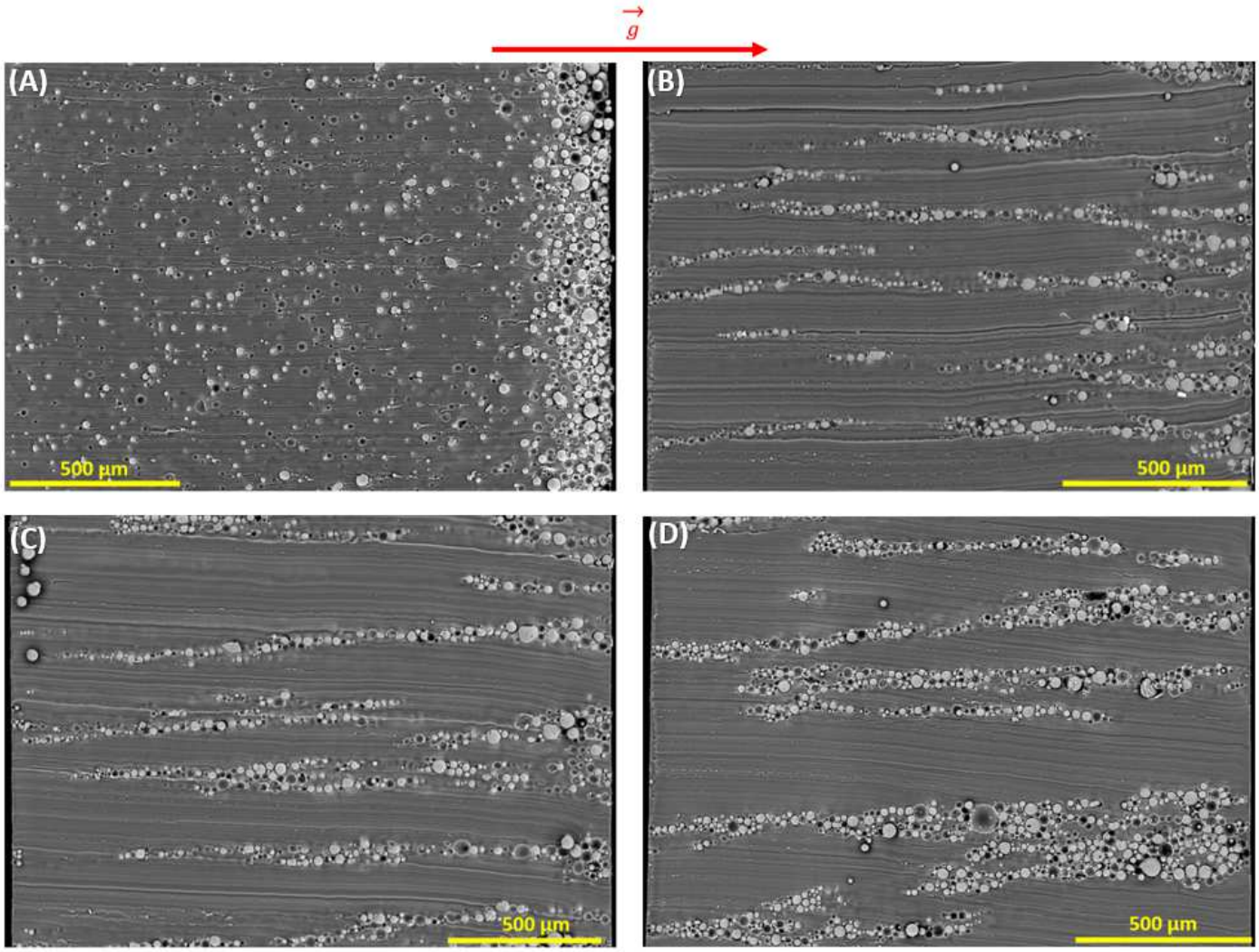

Figure 4 : *SEM cross-sectional micrographs of Al_2O_3/PDMS composites at 10 vol% loading level: (A) 0-3 unstructured sample. (B) Structured sample at a frequency of 100Hz, (C) 10Hz and (D) 1Hz. The electric field used is 4kV.mm^{-1}. ($\vec{g}$ denotes the gravitational acceleration vector, which is along the right-side direction).*

As illustrated on **Figure 4(A)**, the 0-3 unstructured sample exhibits an entirely sedimented structure where high particle concentrations are found in the sample's bottom interface. It is quite evident that such a structure is thermally unfavorable (cf. Section 4.2.2.). **Figures 4(B)**, **(C)** and **(D)** show the cross-sectional observations of 1-3 Al_2O_3/PDMS

composites structured under 4 kV.mm^{-1} at 100 Hz, 10 Hz and 1 Hz, respectively. Both real-time OM and SEM analysis confirmed that fine structural columns coarsen as the frequency decreases. Here, the micrographs indicate the presence of many columns that seem non-percolated. Those discontinuities appear to be more present towards high frequencies. This tendency could highlight another inherent structural influence of the frequency that would not manifest in the transmission OM analysis because of column overlaps. However, given the present data, it can be assumed that the apparent discontinuities are related to the columns not being perfectly in-plane. The cross-sectional observations would therefore capture only the particles located in the same observable plane. Regardless, it can be affirmed that the frequency plays a significant role from a structural perspective, where high frequencies lead to fine thermally conductive pathways as opposed to lower frequencies leading to coarser structures.

Figure 5(A), **(B)**, **(C)** and **(D)** show the cross-sectional SEM observations of the electric field dependence analysis at a fixed frequency of 1 Hz. In accordance with the OM observations, the increasing electric field gives rise to stronger dielectrophoretic force, which tends to reduce the sedimentation effects. Furthermore, the electric field has also an influence over the structure where higher amplitudes lead to larger aligned columns. Because heat transfer by conduction in ceramics is phonon based, phonon/interface scattering is an ever-present phenomenon. In composite materials, more scattering will be present the more fillers-matrix interfaces there are [50]. Hence, a coarser structure with less matrix-filler interfaces ultimately leads to higher conductivities.

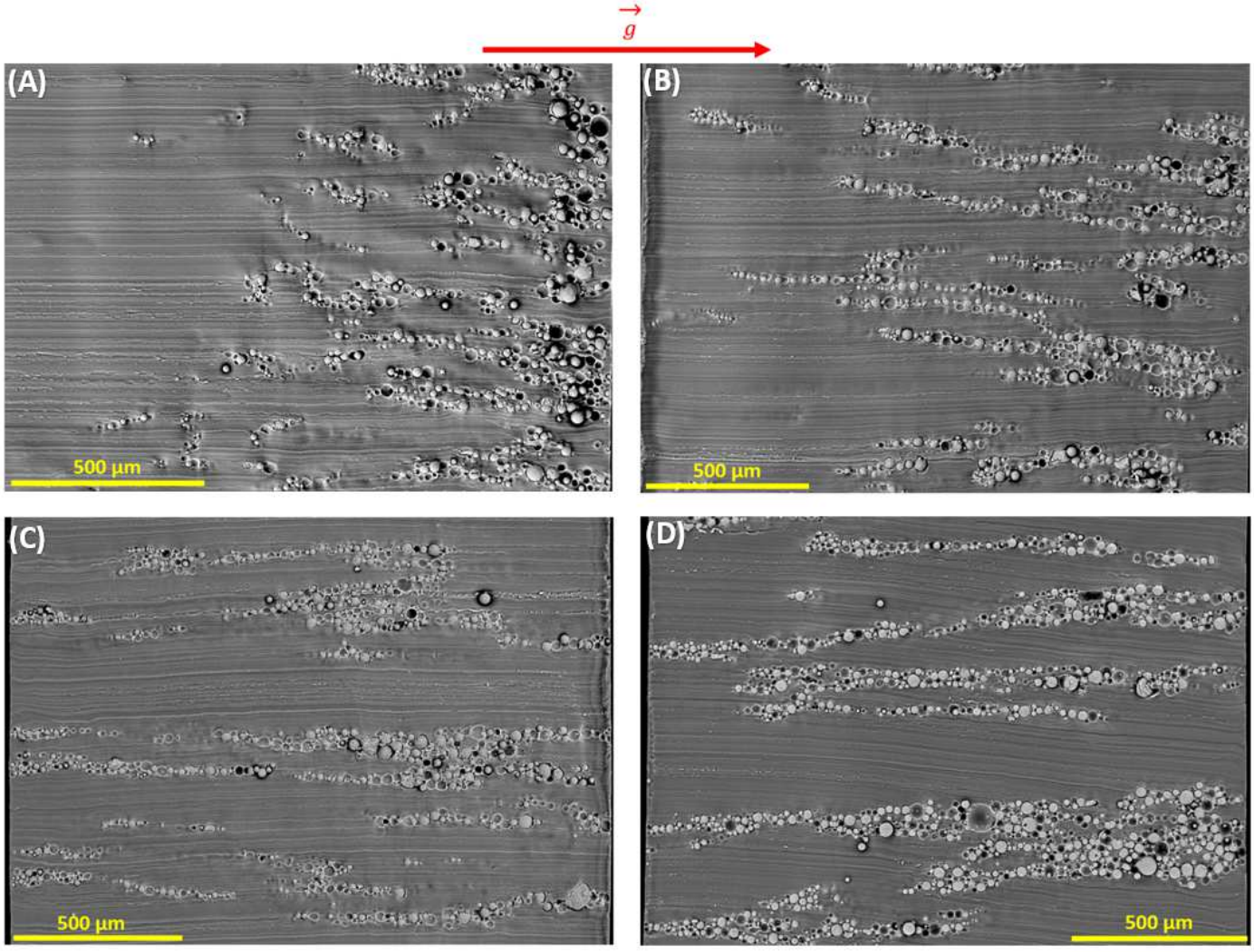

Figure 5 : *SEM cross-sectional micrographs of structured 10vol% Al_2O_3/PDMS composites at a frequency of 1 Hz and an electric field of: (A) 1 kV.mm^{-1}. (B) 2 kV.mm^{-1}. (C) 3 kV.mm^{-1} and (D) 4 kV.mm^{-1}. ($\vec{g}$ denotes the gravitational acceleration vector, which is along the right-side direction).*

To some extent, observations-based OM and SEM images appear slightly different, particularly at 100 Hz. Two main reasons can be outlined as following:

- different technologies of OM and SEM: OM is light transmission based, leading to observation of wide range of columns (around 2mm of thickness). SEM, however, is scanning electron based where only the cross-section interface is observed.
- different loading levels of the tested samples: The sample observed in OM is very low concentration (2,5 vol% of fillers) for light to travel through. Low loading level is more sensible to sedimentation effects due to low viscosity of the blend. The sample observed under SEM contains 10 vol% (i.e., 4 times higher). As the loading level increases, the viscosity increases as well, limiting the sedimentation of the particles.

In spite of different appearances obtained from OM an SEM image, these two techniques allow to achieve the same conclusion: The frequency and the amplitude of the input field significantly affect the structuration as well as the sedimentation effect of the composite. It has been revealed that the best tuning parameters are found equal to 4 kV/mm amplitude and 1 Hz frequency.

4.1.3 Broadband Dielectric Spectroscopy

In order to evaluate the impact of the structuring parameters on dielectric properties of the composites, a broadband dielectric spectroscopy analysis is carried out. **Figure 6(A)** and **(B)** display respectively the real part of the dielectric permittivity as well as the tangent losses of different samples loaded at 10 vol%. The 1-3 composites are structured at a fixed frequency of 1 Hz while the field amplitude varies from 1 to 4 kV.mm^{-1}.

As illustrated in **Figure 6(A),** no matter what the operating frequency is, the real part of permittivity increases with the increasing level of the electric field. Such an enhancement confirms a successful dielectrophoretic alignment under an adequate applied electric field, allowing the formation of columnar pathways with less matrix shielding effects. The 1-3 composite subjected to 4 kV.mm^{-1} displays a 10% increase in permittivity compared to the one randomly dispersed. As a result, dielectrophoretic structuring clearly favors dielectric anisotropy along a preferential direction (i.e., z-axis).

Indeed, as the particles form better columnar pathways, due to less matrix shielding effects, the overall permittivity of the composite increases along the considered direction. Although the real permittivity has been improved through dielectrophoretic alignment, the measured tangent dielectric losses of all samples depicted by **Figure 6(B)** exhibits similar behavior, i.e., close to the value of the pure PDMS. It can therefore be deduced that the proposed approach does not alter the insulating nature of the composites, which is ever so relevant for the intrinsic dielectric strength of those materials.

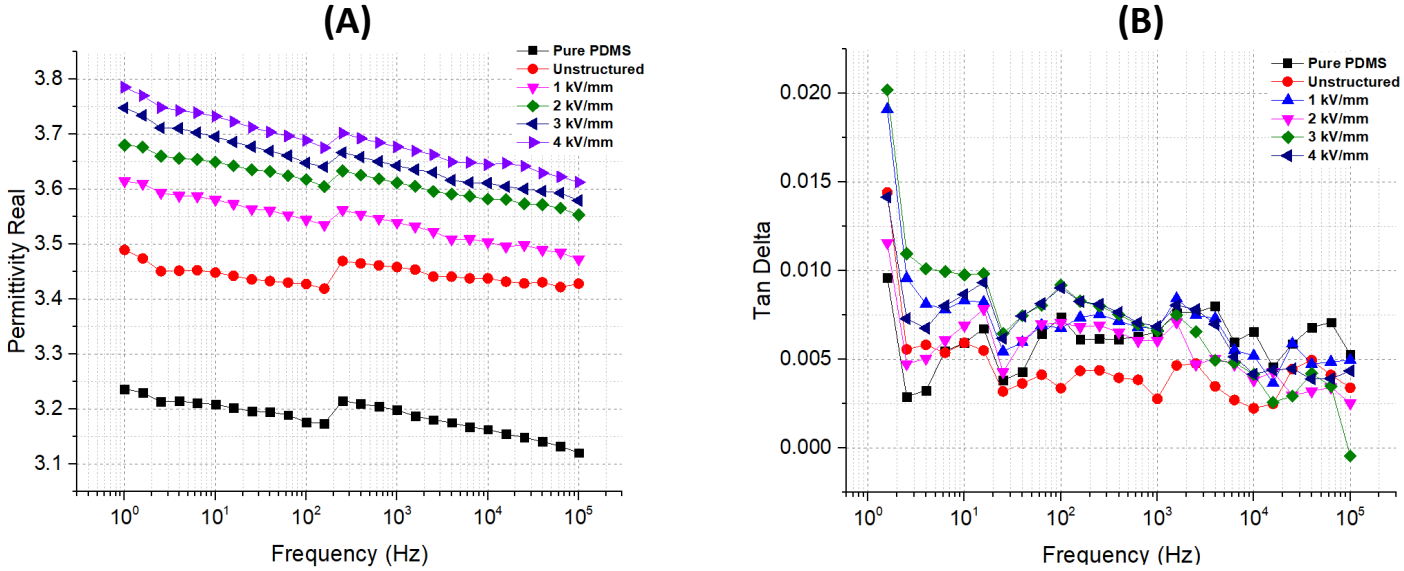

Figure 6 : *Broadband dielectric spectroscopy of 0-3 and 1-3 Al_2O_3/PDMS composites elaborated with 10 vol% concentration along with pure PDMS: (A) Real part of the permittivity; and (B) Dielectric losses. Dielectrophoresis was performed at a 1 Hz frequency and at different field levels ranging from 1 kV.mm^{-1} to 4 kV.mm^{-1}.*

To complete the analysis of **Figure 6**, **Figure 7(A)** and **(B)** illustrate the frequency dependence of the dielectric properties including the relative permittivity and the tangent losses, respectively. The analysis is based on the same composites elaborated with 10 vol% of alumina, subjected to an electric field of 4kV.mm^{-1}.

The results show once again an improvement in the real permittivity as the structuring frequency decreases. This is probably due to the fact that lower frequencies of dielectrophoresis allow a better counterbalance of sedimentation effects (cf., **Figure 5**), as well as coarser and more efficient structures. Finally, the results displayed in **Figure 7(B)** reveals that the broadband dielectric losses remain relatively low and rather close to the values of pure PDMS, regardless of the frequency and amplitude of the electric field used during dielectrophoresis. Accordingly, the structured materials behave as good electric insulators with somewhat enhanced dielectric permittivity.

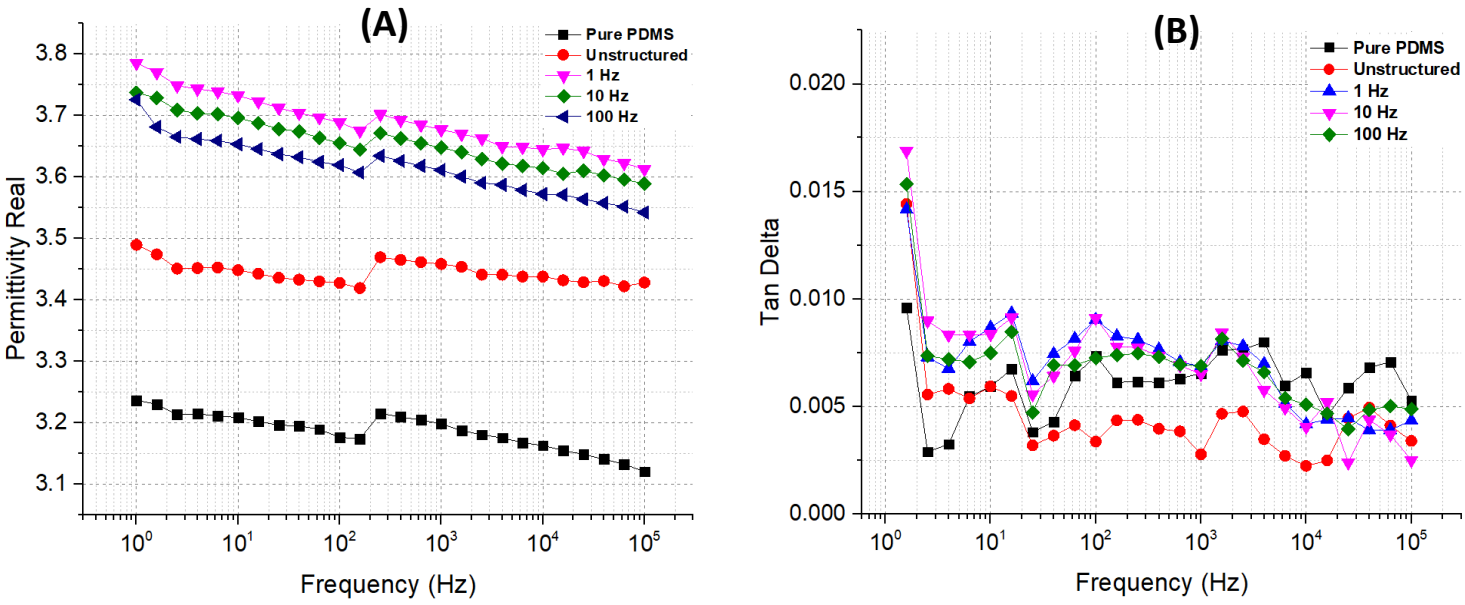

Figure 7 : *Broadband dielectric spectroscopy of 0-3 and 1-3 Al_2O_3/PDMS composites elaborated with 10 vol% concentration along with pure PDMS: (A) Real part of the permittivity. (B) Dielectric losses. Dielectrophoresis was performed at an electric field of 4kV/mm under different frequencies of 1 Hz, 10 Hz and 100 Hz.*

4.1.4 Thermal conductivity

From a fundamental point of view, thermal conduction can be related to two distinguished mechanisms: the movement of charge carriers (electrons or holes) and the oscillation of atoms around their equilibrium point [51], [52]. Thermal conductivity is therefore linked to electrical conductivity (movement of charge carriers) and to the structure of the material (vibrations of atoms). Indeed, in a solid state, the vibrations of atoms are not random and independent of each other, but have proper modes of vibration called "phonons"[53]. These eigenmodes of vibration correspond to waves that can propagate in the material in the case where its structure is periodic and organized. This contribution will therefore be more important in a crystal (ordered), than in a glass (disordered). Mathematically, the thermal conductivity can be expressed as the sum of the contributions of the charge carriers and the vibrations of the atoms in the crystal lattice.

Before addressing the results of this sections, it is relevant to discuss the modified transient plane source (MTPS) method on which the measurement is built. This technique utilizes a one-sided spiral-shaped interfacial heat sensor. A constant electric current is driven through the sensor's spiral that results in a temperature rise at the sample/sensor interface [54]. Given that the electrical resistance of the sensor is dependent on its temperature, by measuring the voltage, the rate at which heat propagates through the tested material can be determined, so can its thermophysical properties.

Any composite material made of two (or more) phases exhibits properties that are dependent on several factors. The intrinsic properties of the present phases and the geometry are undoubtedly the most relevant contributing factors. For homogenously dispersed composites, the effective thermal conductivity (κ) measured through the MTPS method would be equal for both measurable interfaces (i.e., upper and bottom sides). In the case of a sedimented composite however, the two interfaces conduct heat differently, inevitably leading to uneven thermal conductivities. This unbalanced thermal behavior is clearly shown in **Figure 8** where experimental measurements of κ are performed on each interface of the 10 vol% Al_2O_3/PDMS samples (green and red lines). It was expected in **Figure 8(A)** that the bottom-side's thermal conductivity would be higher than the one of the upper-side, especially for the random 0-3 composite (i.e., corresponding to 0 $kV.mm^{-1}$) where the gravitational forces were not compensated by the

dielectrophoretic force. Consequently, a 4-fold difference in the thermal conductivity was recorded between the two interfaces of the 0-3 composite due to higher particle concentrations at the bottom side. This result is perfectly coherent with the SEM analysis described in Subsection 4.1.2. As the electric field increases, the thermal conductivity of both interfaces converges toward the average value with much smaller gaps. For instance, at 4 kV.mm^{-1}, only a 17% variation was recorded between the top and the bottom-side, confirming the consistence of the thermal conductivity along the sample's thickness (i.e., z-direction). **Figure 8(B)** illustrates the structuring frequency effect on the thermal conductivity at a fixed electric field of 4 kV.mm^{-1}, suggesting that the higher the frequency, the more apparent will be the sedimentation effects. In this case, the gap of κ between the two interfaces drastically increases, reaching 1.7-fold and 2.1-fold difference at 10 Hz and 100 Hz, respectively. From a structural standpoint, it is thus pointed out that for a given electric field, a lower frequency (e.g., 1 Hz) is considered more suitable for successfully achieving a better particle structures within the polymer matrix.

As can be predicted by the previous results, the average thermal conductivity (blue lines in **Figure 8**) exhibits a significant improvement (~30%) with the increasing amplitude of the electric field. On the other hand, the average value of κ is quite regular as a function of the frequency, with less than 4% enhancement. In conclusion, the creation of more efficient thermally conductive pathways is carried out under dielectrophoresis at low frequencies and high electric fields (i.e., limited by saturation effects of particle alignment).

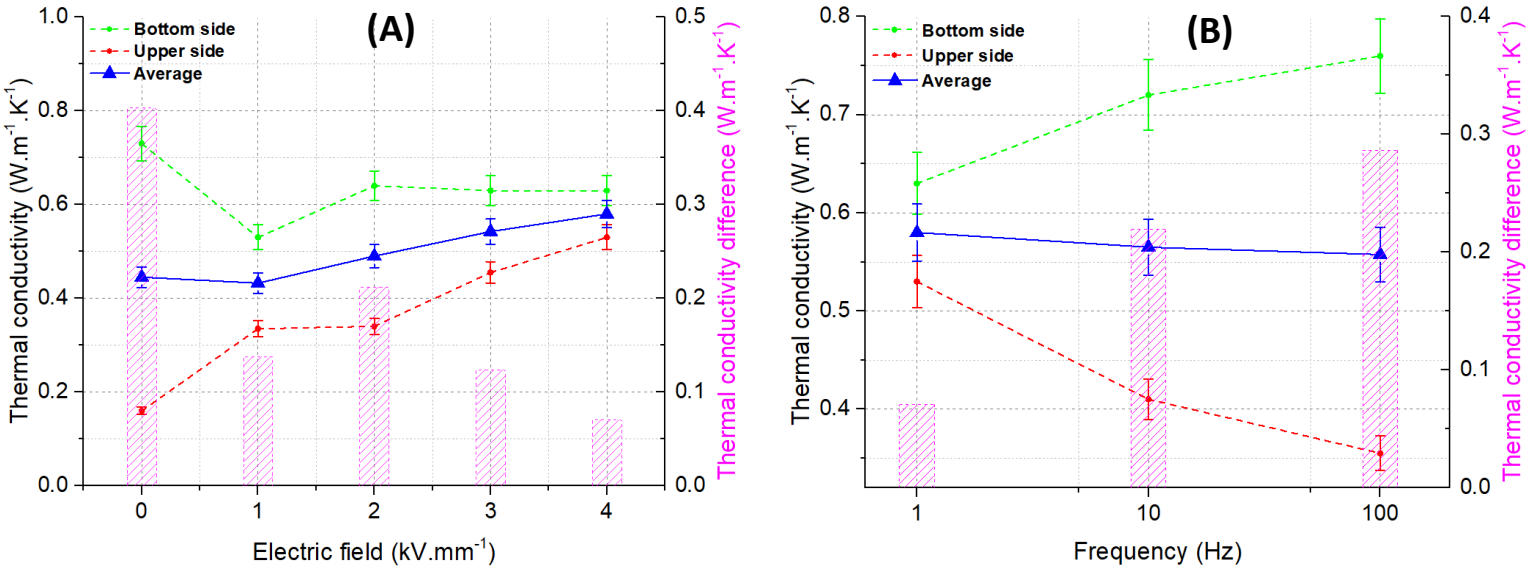

Figure 8 : *Thermal conductivity of 10 vol% Al_2O_3/PDMS as a fuction of different set parameters of the electric field : (A) varying amplitude at a fixed frequency of 1 Hz. (B) varying frequency at a fixed amplitude of 4 kV.mm^{-1}.*

4.2 Dielectrophoresis based performance enhancement

Following the conclusions drawn from the results presented in section 4.1, the chosen parameters for dielectrophoretic structuring process are an electric field of 4 kV.mm^{-1} amplitude and 1 Hz frequency. In order to highlight the alignment effect of Al_2O_3/PDMS composites, different loading levels ranging from 0 vol% to 40 vol% are considered. The dielectric and thermal properties together with the breakdown strength are compared between the 0-3 and the 1-3 structures.

4.2.1 Dielectric property

Figure 9(A) presents the real part of the permittivity for the structured and unstructured samples as a function of the Al_2O_3 volume fraction. It can be observed that whatever is the structural configuration (0-3 or 1-3), the relative permittivity of the Al_2O_3/PDMS composites is almost frequency-independent and increases along with the loading level. As the dielectric permittivity of the Al_2O_3 particles is higher than the one of the PDMS, increasing the particle content will ultimately enhance the overall relative permittivity of the composite, regardless of its structural geometry.

The results also indicate a rather increased relative permittivity of the structured 1-3 samples in comparison with the 0-3 ones particularly under low frequencies. The reason behind the subtle increasing trend is related to the low intrinsic permittivity of Al_2O_3 [55].

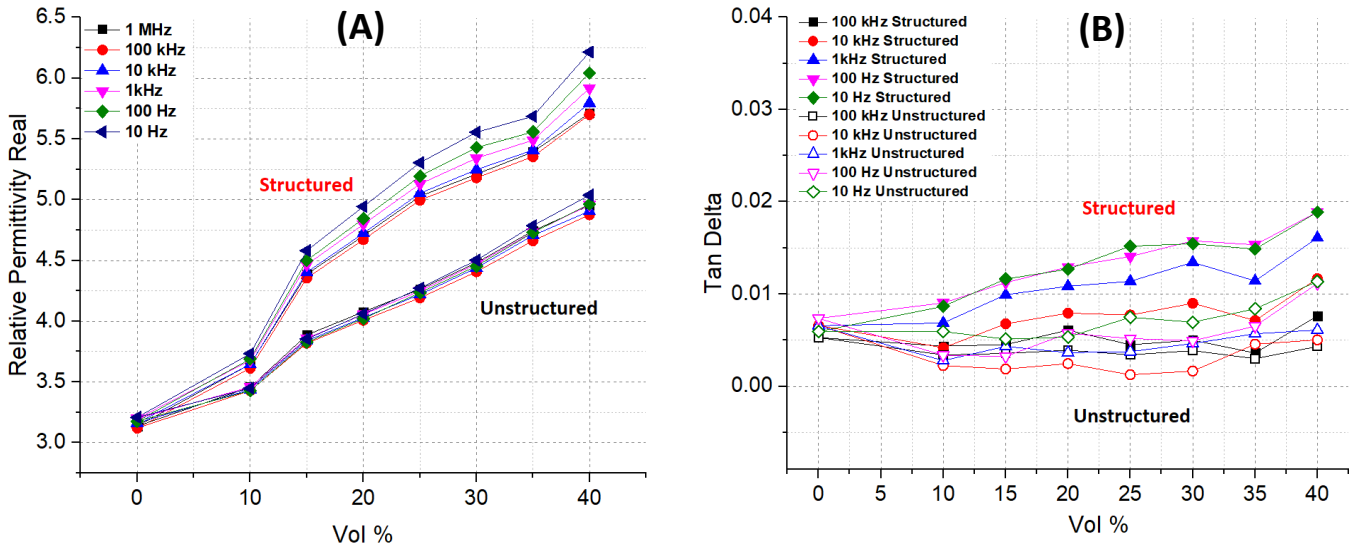

Figure 9 : *Dielectric properties versus the volume fraction of 0-3 and 1-3 Al_2O_3/PDMS composites: (A) Relative permittivity real, (B) Dielectric loss ($tan\delta$).*

Figure 9(B) describes the evolution of the dielectric loss (i.e., $tan\delta$) as a function of Al_2O_3 volume fraction of structured and unstructured samples. Regardless of the volume fraction, the results showed a subtle increase in dielectric losses of the 1-3 composites in comparison with their 0-3 counterparts. The values of $tan\delta$ remain however relatively low for all analyzed samples, suggesting that the dielectrophoretic structuring does not alter their dielectric behavior.

The dielectric permittivity of both structured and unstructured composites is compared to the prediction values of theoretical models. For the 0-3 samples, the Maxwell-Garnet model provides a more accurate fit for spherically shaped fillers. This model is given by [56]:

$$\varepsilon_{eff} = \varepsilon_m \left(\frac{2\varepsilon_m + \varepsilon_p + 2\varphi_p(\varepsilon_p - \varepsilon_m)}{2\varepsilon_m + \varepsilon_p - \varphi_p(\varepsilon_p - \varepsilon_m)} \right) \quad \text{Eq. 4}$$

where ε_{eff} is the effective permittivity of the composite, φ_p is the volume fraction of the particles, ε_m and ε_p are the permittivities of the matrix and the fillers, respectively.

Regarding the 1-3 composites, the parallel dielectric mixing model was used which is based on the General Lichterecker mixing rule. The parallel mixing model is given by [57]:

$$\varepsilon_{eff} = \varphi_p \varepsilon_p + (1 - \varphi_p)\varepsilon_m \quad \text{Eq. 5}$$

The experimental data used for the analysis were measured at a dynamic frequency of 1 MHz. The permittivity of the matrix was fixed at the measured value of 3.13, while the permittivity of particle was varied to better fit the experimental results. As can be seen from **Figure 10(A)** and **(B)**, the experimental measurements of both 0-3 and 1-3 composites compare favorably with their corresponding analytical model. Based on Eq. 4 and 5, predicted permittivity values of Al_2O_3 particles are found within an interval of [9.87, 9.96] which is in agreement with those reported in the literature (i.e., $\varepsilon_{eff} \approx 9.42$) [55].

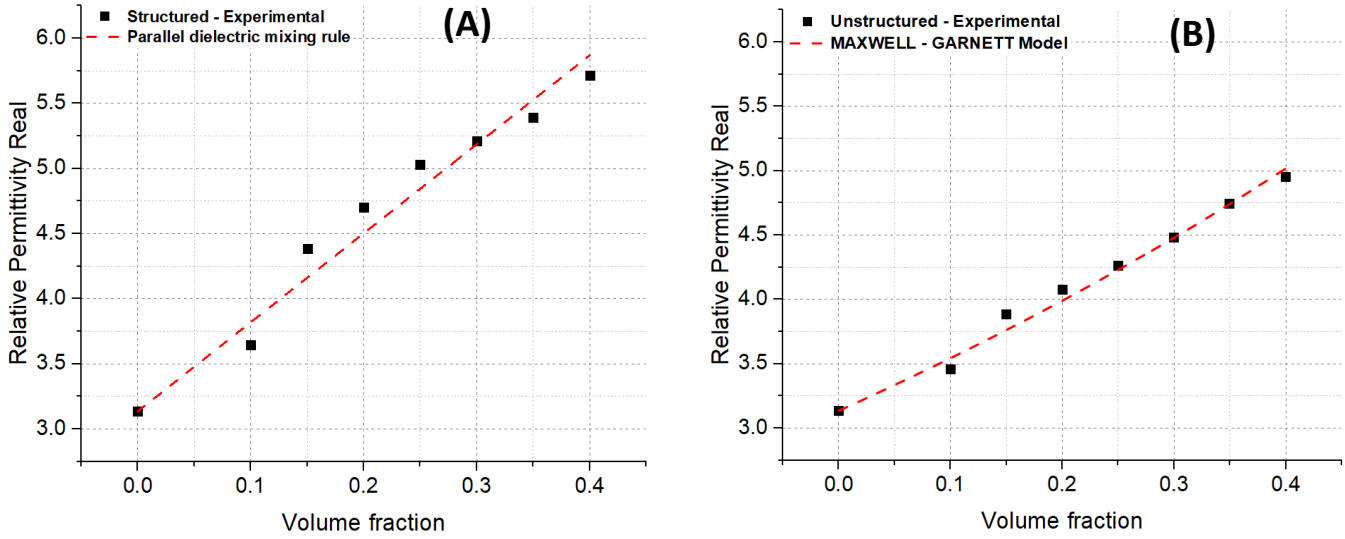

Figure 10 : *Dielectric permittivity of Al_2O_3/PDMS composites as function of the volume fraction: (A) 1-3 composites' experimental data compared to the parallel dielectric mixing law; (B) 0-3 composite's experimental data compared to the Maxwell Garnett Model.*

4.2.2 Thermal property

Figure 11(A) and **(B)** depict the measured thermal conductivity (κ) as a function of the particle content for both structured and unstructured samples respectively. The (κ) values of both sample interfaces (noted upper and bottom side) are displayed, which act as an indicator to how sedimented each sample is. A numerical index (Thermal conductivity difference) is also provided to better describe the thermal conductivity gap between each sample interfaces.

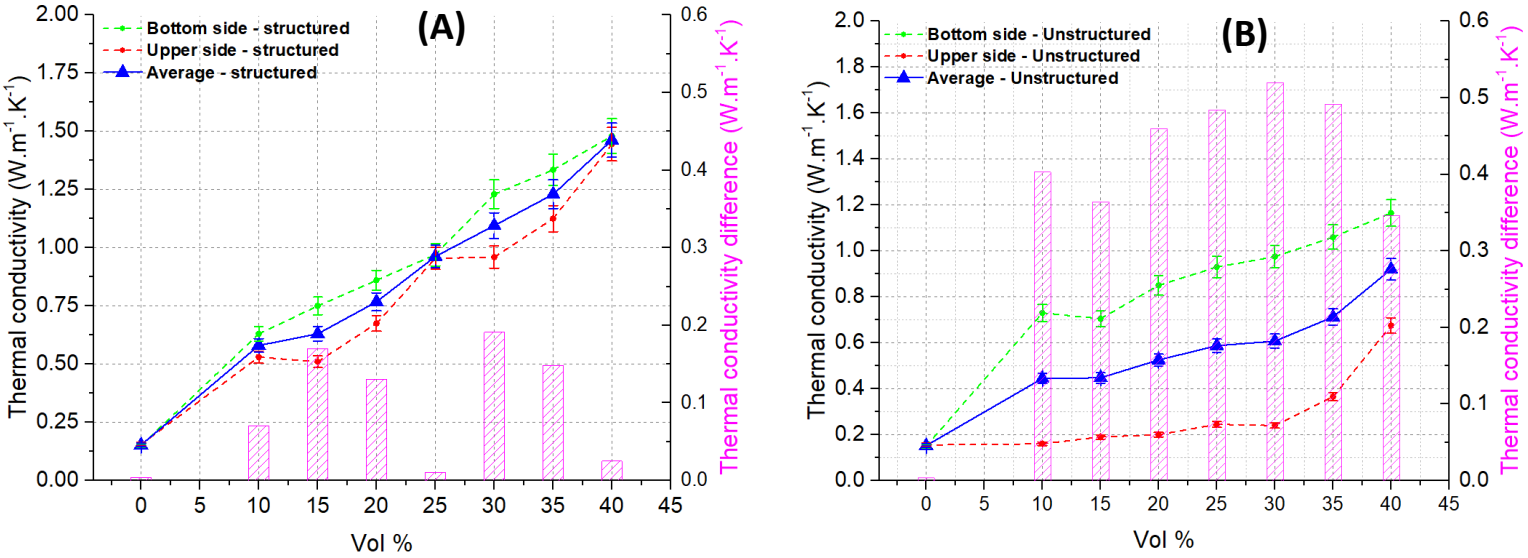

Figure 11 : *Thermal conductivity of Al_2O_3/PDMS in function of the loading level: (A) Samples structured under 4kV.mm^{-1} at 1 Hz and (B) Unstructured samples.*

As clearly illustrated in **Figure 11**, the 1-3 composites exhibit improved thermal properties in contrast with the 0-3 ones, especially at high loading levels. Such an enhancement stems from structured thermally conductive pathways shaped through dielectrophoretic alignment. Similar effects has been observed where a highly anisotropic structure favors thermal conduction along the considered direction [41]. Indeed, not only do the 1-3 structures give rise to a 60% average increase in thermal conductivity, they also overcome the sedimentation consequences that would otherwise be inevitable. The sedimentation effect can be assessed according to the thermal conductivity difference (cf. **Figure 11**), which is twice to five-fold as low in the aligned samples than in the 0-3 ones. This result captures best the

relevance of the dielectrophoretic alignment towards the development of more efficient materials for thermal management.

4.2.3 Dielectric strength

In order to investigate the influence of dielectrophoretic alignment on the materials' dielectric strength, electrical breakdown failures are performed on the Al_2O_3/PDMS composites elaborated with different loading levels. All samples, with the same thickness of 1 mm, are subjected to an increasing voltage rate of 500 $V.s^{-1}$ until the breakdown occurs. The experimental test is replicated 20 times on each sample to ensure enough statistical power. The breakdown probability is then determined through the exponential Weibull function expressed as follows [58], [59], [60]:

$$P(E) = 1 - \exp\left[-\left(\frac{E}{\lambda}\right)^{k}\right] \qquad \text{Eq. 6}$$

where $P(E)$ is the breakdown probability, E is the electric field, λ is the scale parameter characterizing the electric field at 63.2% breakdown probability, and k is the data distribution or the standard deviation of the experiment.

Figure 12(A) and (B) display the empirical breakdown probability versus the electric field for structured and unstructured samples, respectively.

For both 0-3 and 1-3 structural connectivity, the breakdown probability increases with the applied electric field, reflecting its coherence with the Weibull model of Eq. 6. Regardless of the loading level, the results show a similar breakdown behavior between 0-3 and 1-3 samples. Indeed, as the dielectric losses of the structured samples are relatively close to the unstructured ones (cf. **Figure 9(B)**), no major shifts in the dielectric strength have been observed. The fact is that both the PDMS matrix and the alumina ceramic particles have good insulating properties. Therefore, their sedimentation state did not prove to be as relevant to the dielectric strength as it was to thermal properties. In essence, the developed materials are considered to be excellent insulators that can support a higher input electric field than 40 $kV.mm^{-1}$, under which 63.2% breakdown probability would occur. Since the gap in dielectric permittivity between the alumina particles and the PDMS polymer is not substantial (only 3-fold difference), the distributed electric field across the two phases (filler and matrix) is not highly unbalanced [43], [59]. According to the conservation of the electric charge displacement (i.e., $D = \varepsilon E$), the electric field's level is more concentrated in phase presenting a lower permittivity (i.e., polymer matrix). As the fillers' permittivity increases, the electric field's amplitude grows bigger in the polymer matrix until reaching its dielectric strength where the electrical breakdown occurs. The breakdown probability is also revealed to increase with the sample's thickness. In the considered application where a significant thickness is necessary for thermal management (high thermal inertia), choosing an adequate coupling of fillers and matrix (alumina and silicone) allows to achieve composites with a satisfactory breakdown strength, even at high sample thickness (e.g., 1 mm). Furthermore, dielectrophoresis applied to Al_2O_3/PDMS composites leads to higher material performance in term of dielectric and thermal properties, without changing its dielectric strength.

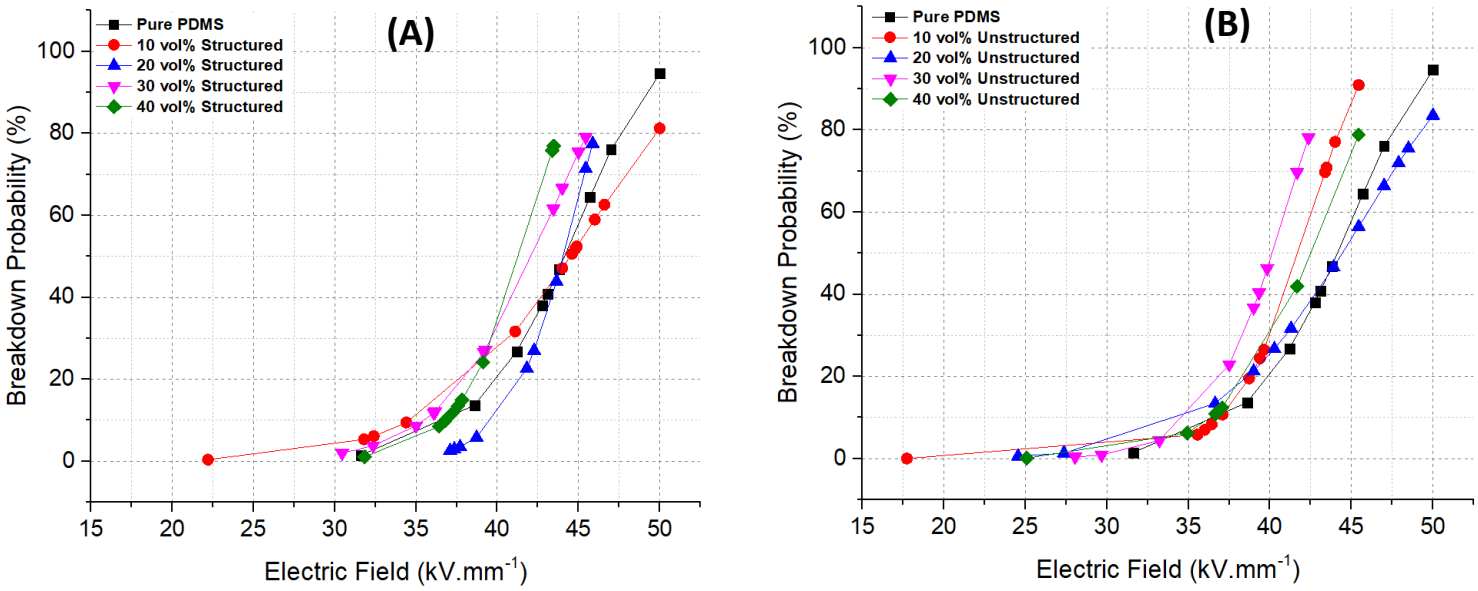

Figure 12 : *Breakdown probability versus the electric field applied to Al_2O_3/PDMS composites at different loading levels: (A) 1-3 Structured samples; and (B) 0-3 Unstructured samples.*

5 Conclusion

This work focused on the effect of dielectrophoretic alignment on thermo-composites with a particular attention to the relationship between relevant parameters and the sedimentation state of the fillers. This often-overlooked aspect of composite fabrication has proven to be an efficient and simple approach to substantially improve the material properties. The effect of structuring parameters including amplitude and frequency of the applied electric field was investigated to determine the best configuration for dielectrophoretic process. Through microscopic observations (SEM, OM), particle alignment along the field direction was proven to be successfully achieved in a non-cured state of the composites. These results clearly show major consequences of sedimentation on the random 0-3 samples, as opposed to the aligned ones, where the dielectrophoretic force allows to counterbalance the effect of gravity. Based on several characterization tests, experimental results pointed out that a low frequency (1 Hz) and high amplitude (4 $kV.mm^{-1}$) of the input electric field were the most efficient conditions. These parameters were utilized to structure a various range of filler content (i.e., 10 to 40 vol%) for a comparison between 1-3 and 0-3 connectivity patterns. The thermal conductivity, dielectric properties together with the structural sedimentation were successfully improved through dielectrophoretic alignment while keeping the dielectric losses and dielectric strength unchanged. Such structuring process has therefore the potential to lead to cheaper, lighter and more efficient thermally conductive composites.

Acknowledgements

All the authors acknowledge the financial support from the GETELEC company, the Institute Carnot, and the "Bonus Quality Innovation" (BQI) from INSAVALOR. The authors also thank "Région Auvergne Rhone Alpes".

Conflict of Interest:
The authors declare no conflict of interest.

Author Contribution

O.Z. wrote the manuscript. O.Z., F.G., G.D'A and M.Q.L reviewed and edited the manuscript. O.Z. elaborated the composites. O.Z., F.G. and G.D'A performed the materials' characterization. O.Z., G.D'A, P.J.C, F.G. and J.F.C. analyzed the data. P.J.C, G.C and J.F.C, provided some help on experimental setups. This work was supervised by P.J.C, J.F.C and F.G.

Keywords

Dielectrophoresis, sedimentation effects, structuring parameters, thermally conductive composites, thermal management, properties enhancement.

References

[1] I. Paper, A. Bar-cohen, in 1985 To 1.0 Cm in 1990 and Can Be, 1739 (1995).
[2] A.L. Moore, L. Shi, Emerging challenges and materials for thermal management of electronics, Materials Today. 17 (2014) 163–174. https://doi.org/10.1016/j.mattod.2014.04.003.
[3] B.Y.M.M. Waldrop, O.F.M.S. Law, M. Interesting, More Than Will Soon Abandon Its Pursuit, Nature. 530 (2016) 145.
[4] K.K. Guosheng Jiang, Liyong Diao, Advanced Thermal Management Materials, (n.d.). https://doi.org/10.1109/TCPMT.2017.2661700.
[5] Z. Xiang, B. Ducharne, N. Della Schiava, J.F. Capsal, P.J. Cottinet, G. Coativy, P. Lermusiaux, M.Q. Le, Induction heating-based low-frequency alternating magnetic field: High potential of ferromagnetic composites for medical applications, Materials and Design. 174 (2019) 107804. https://doi.org/10.1016/j.matdes.2019.107804.
[6] D.D.L. Chung, Applied Materials Science, 2001. https://doi.org/10.1201/9781420040975.
[7] J.P. Gwinn, R.L. Webb, Performance and testing of thermal interface materials, Microelectronics Journal. 34 (2003) 215–222. https://doi.org/10.1016/S0026-2692(02)00191-X.
[8] T. Schubert, B. Trindade, T. Weißg, B. Kieback, Interfacial design of Cu-based composites prepared by powder metallurgy for heat sink applications, 475 (2008) 39–44. https://doi.org/10.1016/j.msea.2006.12.146.
[9] Z. Su, H. Wang, J. He, Y. Guo, Q. Qu, X. Tian, Fabrication of Thermal Conductivity Enhanced Polymer Composites by Constructing an Oriented Three-Dimensional Staggered Interconnected Network of Boron Nitride Platelets and Carbon Nanotubes, ACS Applied Materials and Interfaces. 10 (2018) 36342–36351. https://doi.org/10.1021/acsami.8b09703.
[10] X. Huang, P. Jiang, T. Tanaka, A review of dielectric polymer composites with high thermal conductivity, IEEE Electrical Insulation Magazine. 27 (2011) 8–16. https://doi.org/10.1109/MEI.2011.5954064.
[11] J. Chen, X. Huang, B. Sun, P. Jiang, Highly Thermally Conductive Yet Electrically Insulating Polymer/Boron Nitride Nanosheets Nanocomposite Films for Improved Thermal Management Capability, ACS Nano. 13 (2019) 337–345. https://doi.org/10.1021/acsnano.8b06290.
[12] B.C. Zhi, Y. Bando, T. Terao, C. Tang, H. Kuwahara, D. Golberg, Towards Thermoconductive , Electrically Insulating Polymeric Composites with Boron Nitride Nanotubes as Fillers, (2009) 1857–1862. https://doi.org/10.1002/adfm.200801435.
[13] M.J. Biercuk, M.C. Llaguno, M. Radosavljevic, J.K. Hyun, A.T. Johnson, J.E. Fischer, Carbon nanotube composites for thermal management, Applied Physics Letters. 80 (2002) 2767–2769. https://doi.org/10.1063/1.1469696.
[14] T. Goto, M. Iida, H. Tan, C. Liu, K. Mayumi, R. Maeda, K. Kitahara, K. Hatakeyama, T. Ito, Y. Shimizu, H. Yokoyama, K. Kimura, K. Ito, Y. Hakuta, K. Terashima, Thermally conductive tough flexible elastomers as composite of slide-ring materials and surface modified boron nitride particles via plasma in solution, Applied Physics Letters. 112 (2018). https://doi.org/10.1063/1.5020325.
[15] P.-J. Cottinet, M.-Q. Le, J. Degraff, C. Souders, Z. Liang, B. Wang, C. Zhang, Strain phenomenon in carbon nanotube buckpaper actuator: Experiments and modeling, Sensors and Actuators A: Physical. 194 (2013) 252–258. https://doi.org/10.1016/j.sna.2013.02.014.
[16] Z.G. Wang, M.Z. Chen, Y.H. Liu, H.J. Duan, L. Xu, L. Zhou, J.Z. Xu, J. Lei, Z.M. Li, Nacre-like composite films with high thermal conductivity, flexibility, and solvent stability for thermal management applications, Journal of Materials Chemistry C. 7 (2019) 9018–9024. https://doi.org/10.1039/c9tc02845e.
[17] C. Zweben, Advances in composite materials for thermal management in electronic packaging, Jom. 50 (1998) 47–51. https://doi.org/10.1007/s11837-998-0128-6.
[18] J. Gu, Z. Lv, Y. Wu, Y. Guo, L. Tian, H. Qiu, W. Li, Q. Zhang, Dielectric thermally conductive boron nitride/polyimide composites with outstanding thermal stabilities via in-situ polymerization-electrospinning-hot press method, Composites Part A: Applied Science and Manufacturing. 94 (2017) 209–216. https://doi.org/10.1016/j.compositesa.2016.12.014.
[19] X. Huang, C. Zhi, Y. Lin, H. Bao, G. Wu, P. Jiang, Y.W. Mai, Thermal conductivity of graphene-based polymer nanocomposites, Materials Science and Engineering R: Reports. 142 (2020) 100577. https://doi.org/10.1016/j.mser.2020.100577.

[20] P.J.F. Harris, Carbon nanotube composites, International Materials Reviews. 49 (2004) 31–43. https://doi.org/10.1179/095066004225010505.
[21] R. Andrews, M.C. Weisenberger, Carbon nanotube polymer composites, Current Opinion in Solid State and Materials Science. 8 (2004) 31–37. https://doi.org/10.1016/j.cossms.2003.10.006.
[22] K. Ruan, X. Shi, Y. Guo, J. Gu, Interfacial thermal resistance in thermally conductive polymer composites: A review, Composites Communications. 22 (2020) 100518. https://doi.org/10.1016/j.coco.2020.100518.
[23] H. Zhang, X. Zhang, D. Li, X. Yang, D. Wu, J. Sun, Thermal conductivity enhancement via conductive network conversion from “sand-like” to “stone-like” in the polydimethylsiloxane composites, Composites Communications. 22 (2020) 100509. https://doi.org/10.1016/j.coco.2020.100509.
[24] T. Shimizu, R. Kishi, K. Kobashi, T. Morimoto, T. Okazaki, T. Yamada, K. Hata, Improved thermal stability of silicone rubber nanocomposites with low filler content, achieved by well-dispersed carbon nanotubes, Composites Communications. 22 (2020) 100482. https://doi.org/10.1016/j.coco.2020.100482.
[25] Z. Xiang, M.Q. Le, P.J. Cottinet, P. Griffiths, G.P. Baeza, J.F. Capsal, P. Lermusiaux, N. Della Schiava, B. Ducharne, Development of anisotropic ferromagnetic composites for low-frequency induction heating technology in medical applications, Materials Today Chemistry. 19 (2021). https://doi.org/10.1016/j.mtchem.2020.100395.
[26] X. Zhang, M.Q. Le, V.C. Nguyen, J.F. Mogniotte, J.F. Capsal, D. Grinberg, P.J. Cottinet, L. Petit, Characterization of micro-ZnO/PDMS composite structured via dielectrophoresis – Toward medical application, Materials and Design. 208 (2021) 109912. https://doi.org/10.1016/j.matdes.2021.109912.
[27] R. Ramalingame, N. Udhayakumar, R. Torres, I.T. Neckel, C. Müller, O. Kanoun, MWCNT-PDMS Nanocomposite Based Flexible Multifunctional Sensor for Health Monitoring, Procedia Engineering. 168 (2016) 1775–1778. https://doi.org/10.1016/j.proeng.2017.02.003.
[28] G. D’Ambrogio, O. Zahhaf, M. Bordet, M.Q. Le, N. Della Schiava, R. Liang, P.-J. Cottinet, J.-F. Capsal, Structuring BaTiO3 /PDMS nanocomposite via dielectrophoresis for fractional flow reserve measurement, Advanced Engineering Materials. adem.202100341 (2021). https://doi.org/10.1002/adem.202100341.
[29] H. Chen, V. V. Ginzburg, J. Yang, Y. Yang, W. Liu, Y. Huang, L. Du, B. Chen, Thermal conductivity of polymer-based composites: Fundamentals and applications, Progress in Polymer Science. 59 (2016) 41–85. https://doi.org/10.1016/j.progpolymsci.2016.03.001.
[30] Q. Li, C. Liu, S. Fan, Thermal boundary resistances of carbon nanotubes in contact with metals and polymers, Nano Letters. 9 (2009) 3805–3809. https://doi.org/10.1021/nl901988t.
[31] M.J. Yoo, D.S. Seo, S.H. Kim, W.S. Lee, T.G. Seong, S.H. Kweon, B.J. Jeong, Y.H. Jeong, S. Nahm, Electric field assembled anisotropic alumina composite for thermal dissipation applications, Journal of Composite Materials. 48 (2014) 201–208. https://doi.org/10.1177/0021998312469993.
[32] X. Zeng, J. Sun, Y. Yao, R. Sun, J. Xu, C. Wong, A Combination of Boron Nitride Nanotubes and Cellulose Nano fi bers for the Preparation of a Nanocomposite with High Thermal Conductivity, (2017). https://doi.org/10.1021/acsnano.7b02359.
[33] K. Kim, H. Ju, J. Kim, Filler orientation of boron nitride composite via external electric field for thermal conductivity enhancement, Ceramics International. 42 (2016) 8657–8663. https://doi.org/10.1016/j.ceramint.2016.02.098.
[34] C.A. Randall, S. Miyazaki, K.L. More, A.S. Bhalla, R.E. Newnham, Structural-property relationships in dielectrophoretically assembled BaTiO3 nanocomposites, Materials Letters. 15 (1992) 26–30. https://doi.org/10.1016/0167-577X(92)90006-6.
[35] J. Blair, M.G. Lacy, from the SAGE Social Science Collections . Rights Reserved ., Sociological Methods & Research. 28 (2000) 251–280. https://doi.org/10.1177/016344300022005001.
[36] K. Kim, H. Ju, J. Kim, Vertical particle alignment of boron nitride and silicon carbide binary filler system for thermal conductivity enhancement, Composites Science and Technology. 123 (2016) 99–105. https://doi.org/10.1016/j.compscitech.2015.12.004.
[37] Y. Han, S. Lv, C. Hao, F. Ding, Y. Zhang, Thermal conductivity enhancement of BN/silicone composites cured under electric field: Stacking of shape, thermal conductivity, and particle packing structure anisotropies, Thermochimica Acta. 529 (2012) 68–73. https://doi.org/10.1016/j.tca.2011.11.029.
[38] G. D’Ambrogio, O. Zahhaf, M.-Q. Le, J.-F. Capsal, P.-J. Cottinet, Dielectrophoresis Structurization of PZT/PDMS Micro-Composite for Elastronic Function: Towards Dielectric and Piezoelectric Enhancement, Materials. 14 (2021) 4071. https://doi.org/10.3390/ma14154071.
[39] A. Munaz, M.J.A. Shiddiky, N.-T. Nguyen, Recent advances and current challenges in magnetophoresis based micro magnetofluidics, Biomicrofluidics. 12 (2018) 031501. https://doi.org/10.1063/1.5035388.
[40] K. Kim, J. Kim, Magnetic aligned AlN/epoxy composite for thermal conductivity enhancement at low filler content, Composites Part B: Engineering. 93 (2016) 67–74. https://doi.org/10.1016/j.compositesb.2016.02.052.

[41] Z. Xiang, V. Nguyen, B. Ducharne, N. Della Schiava, J. Capsal, P. Cottinet, M. Le, 3D Printing of Flexible Composites via Magnetophoresis: Toward Medical Application Based on Low-Frequency Induction Heating Effect, Macromolecular Materials and Engineering. (2021) 2100211. https://doi.org/10.1002/mame.202100211.
[42] H.A. Pohl, The motion and precipitation of suspensoids in divergent electric fields, Journal of Applied Physics. 22 (1951) 869–871. https://doi.org/10.1063/1.1700065.
[43] X. Zhang, M.Q. Le, O. Zahhaf, J.F. Capsal, P.J. Cottinet, L. Petit, Enhancing dielectric and piezoelectric properties of micro-ZnO/PDMS composite-based dielectrophoresis, Materials and Design. 192 (2020) 108783. https://doi.org/10.1016/j.matdes.2020.108783.
[44] G. D'Ambrogio, O. Zahhaf, Y. Hebrard, M.Q. Le, P.-J. Cottinet, J.-F. Capsal, Micro-Structuration of Piezoelectric Composites Using Dielectrophoresis: Toward Application in Condition Monitoring of Bearings, Advanced Engineering Materials. 23 (2021) 2000773. https://doi.org/10.1002/adem.202000773.
[45] C. Park, R.E. Robertson, Alignment of particles by an electric field, Materials Science and Engineering A. 257 (1998) 295–311. https://doi.org/10.1016/S0921-5093(98)00848-X.
[46] R.E. Newnham, D.P. Skinner, L.E. Cross, Connectivity and piezoelectric-pyroelectric composites, Materials Research Bulletin. 13 (1978) 525–536. https://doi.org/10.1016/0025-5408(78)90161-7.
[47] C-Therm, Modified Transient Plane Source (MTPS): Theory of Operation, (n.d.) 1–10.
[48] C. Park, R.E. Robertson, Aligned microstructure of some particulate polymer composites obtained with an electric field, Journal of Materials Science. 33 (1998) 3541–3553. https://doi.org/10.1023/A:1004638825477.
[49] C.P. Bowen, T.R. Shrout, R.E. Newnham, C.A. Randall, A study of the frequency dependence of the dielectrophoretic effect in thermoset polymers, Journal of Materials Research. 12 (1997) 2345–2356. https://doi.org/10.1557/JMR.1997.0311.
[50] N. Burger, A. Laachachi, M. Ferriol, M. Lutz, V. Toniazzo, D. Ruch, Progress in Polymer Science Review of thermal conductivity in composites : Mechanisms , parameters and theory, Progress in Polymer Science. 61 (2016) 1–28. https://doi.org/10.1016/j.progpolymsci.2016.05.001.
[51] L. Zhang, H. Deng, Q. Fu, Recent progress on thermal conductive and electrical insulating polymer composites, Composites Communications. 8 (2018) 74–82. https://doi.org/10.1016/j.coco.2017.11.004.
[52] X. Yang, C. Liang, T. Ma, Y. Guo, J. Kong, J. Gu, M. Chen, J. Zhu, A review on thermally conductive polymeric composites: classification, measurement, model and equations, mechanism and fabrication methods, Advanced Composites and Hybrid Materials. 1 (2018) 207–230. https://doi.org/10.1007/s42114-018-0031-8.
[53] X. Wan, D. Ma, D. Pan, L. Yang, N. Yang, Optimizing thermal transport in graphene nanoribbon based on phonon resonance hybridization, Materials Today Physics. 20 (2021) 100445. https://doi.org/10.1016/j.mtphys.2021.100445.
[54] A. Harris, S. Kazachenko, R. Bateman, J. Nickerson, M. Emanuel, Measuring the thermal conductivity of heat transfer fluids via the modified transient plane source (MTPS), Journal of Thermal Analysis and Calorimetry. 116 (2014) 1309–1314. https://doi.org/10.1007/s10973-014-3811-6.
[55] K.Z. Rajab, M. Naftaly, E.H. Linfield, J.C. Nino, D. Arenas, D. Tanner, R. Mittra, M. Lanagan, Broadband dielectric characterization of aluminum oxide (Al 2O3), Journal of Microelectronics and Electronic Packaging. 5 (2008) 2–7. https://doi.org/10.4071/1551-4897-5.1.1.
[56] F. Achard, James clerk maxwell, a treatise on electricity and magnetism, first edition (1873), Landmark Writings in Western Mathematics 1640-1940. (2005) 564–587. https://doi.org/10.1016/B978-044450871-3/50125-X.
[57] Y. Wu, X. Zhao, F. Li, Z. Fan, Evaluation of mixing rules for dielectric constants of composite dielectrics by MC-FEM calculation on 3D cubic lattice, Journal of Electroceramics. 11 (2003) 227–239. https://doi.org/10.1023/B:JECR.0000026377.48598.4d.
[58] K. Thetpraphi, S. Chaipo, W. Kanlayakan, P.J. Cottinet, M.Q. Le, L. Petit, D. Audigier, J. Kuhn, G. Moretto, J.F. Capsal, Advanced Plasticized Electroactive Polymers Actuators for Active Optical Applications: Live Mirror, Advanced Engineering Materials. 22 (2020) 1–11. https://doi.org/10.1002/adem.201901540.
[59] F. Pedroli, A. Flocchini, A. Marrani, M.Q. Le, O. Sanseau, P.J. Cottinet, J.F. Capsal, Boosted energy-storage efficiency by controlling conduction loss of multilayered polymeric capacitors, Materials and Design. 192 (2020) 108712. https://doi.org/10.1016/j.matdes.2020.108712.
[60] F. Pedroli, A. Marrani, M.Q. Le, C. Froidefond, P.J. Cottinet, J.F. Capsal, Processing optimization: A way to improve the ionic conductivity and dielectric loss of electroactive polymers, Journal of Polymer Science, Part B: Polymer Physics. 56 (2018) 1164–1173. https://doi.org/10.1002/polb.24636.

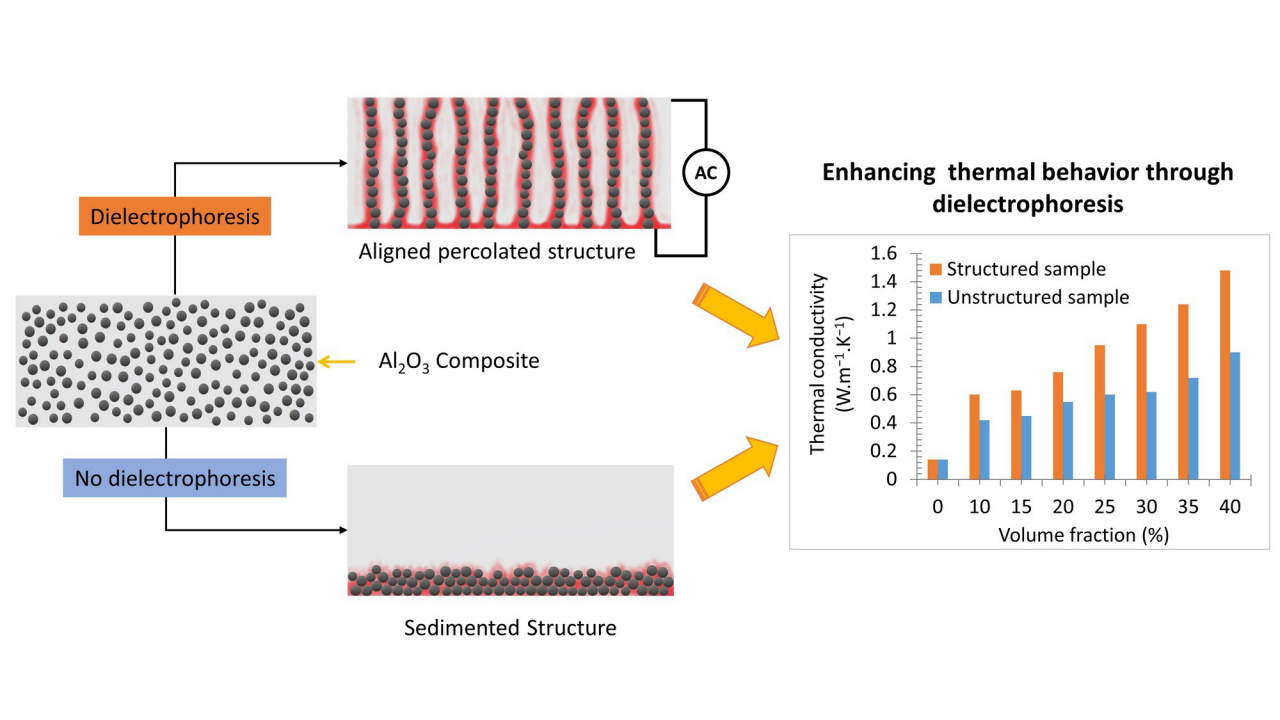
Dielectrophoresis
AC
Aligned percolated structure
Al_2O_3 Composite
No dielectrophoresis
Sedimented Structure
Enhancing thermal behavior through dielectrophoresis
Thermal conductivity (W.m^{-1}.K^{-1})
Structured sample
Unstructured sample
1.6
1.4
1.2
1
0.8
0.6
0.4
0.2
0
0 10 15 20 25 30 35 40
Volume fraction (%)